Cerebral Cortex March 2010;20:730–742
doi:10.1093/cercor/bhp138
Advance Access publication July 20, 2009

Broca's Area Homologue in Chimpanzees (*Pan troglodytes*): Probabilistic Mapping, Asymmetry, and Comparison to Humans

Natalie M. Schenker[1], William D. Hopkins[2,3], Muhammad A. Spocter[1], Amy R. Garrison[1], Cheryl D. Stimpson[1], Joseph M. Erwin[4,5], Patrick R. Hof[6,7] and Chet C. Sherwood[1]

[1]Department of Anthropology, The George Washington University, Washington, DC 20052, USA, [2]Department of Psychology, Agnes Scott College, Decatur, GA 30030, USA, [3]Division of Psychobiology, Yerkes National Primate Research Center, Atlanta, GA 30322, USA, [4]Division of Biomedical Sciences and Pathobiology, Virginia-Maryland Regional College of Veterinary Medicine at Virginia Polytechnic Institute and State University, Blacksburg, VA 24036, USA, [5]Foundation for Comparative and Conservation Biology, Needmore, PA 17238, USA, [6]Department of Neuroscience, Mount Sinai School of Medicine, New York, NY 10029, USA and [7]New York Consortium in Evolutionary Primatology, New York, NY, USA

Neural changes that occurred during human evolution to support language are poorly understood. As a basis of comparison to humans, we used design-based stereological methods to estimate volumes, total neuron numbers, and neuron densities in Brodmann's areas 44 and 45 in both cerebral hemispheres of 12 chimpanzees (*Pan troglodytes*), one of our species' closest living relatives. We found that the degree of interindividual variation in the topographic location and quantitative cytoarchitecture of areas 44 and 45 in chimpanzees was comparable to that seen in humans from previous studies. However, in contrast to the documented asymmetries in humans, we did not find significant population-level hemispheric asymmetry for any measures of areas 44 and 45 in chimpanzees. Furthermore, there was no relationship between asymmetries of stereological data and magnetic resonance imaging–based measures of inferior frontal gyrus morphology or hand preference on 2 different behavioral tasks. These findings suggest that Broca's area in the left hemisphere expanded in relative size during human evolution, possibly as an adaptation for our species' language abilities.

Keywords: cytoarchitecture, evolution, great ape, handedness, stereology

Introduction

Among animal communication systems, human language is distinctive for its combinatorial capacity and hierarchical syntactic structure (Hauser et al. 2002). A principal node in the cortical language network is Broca's area, which encompasses part of the inferior frontal lobe that includes Brodmann's cytoarchitectonic areas 44 and 45 (Amunts et al. 1999; Keller et al. 2009). This region is involved in language production and comprehension (Ojemann 1991; Burton 2001; Caplan 2001; Foundas 2001; Bookheimer 2002), as well as nonlinguistic memory processes (Cabeza and Nyberg 2000; Aboitiz et al. 2006) and ordering of hierarchical dependencies in sequences (Friederici et al. 2006). It also participates in mirror neuron networks that are shared in common by humans and other primates, such as macaque monkeys (Fadiga and Craighero 2006). Recent evidence indicates that, like humans, the inferior frontal cortex of nonhuman primates may be similarly involved in processing communication signals. Specifically, perception of species-specific vocalizations and facial expressions activates the inferior frontal cortex in macaque monkeys (Ferrari et al. 2003; Gil-da-Costa et al. 2006), whereas the production of communicative hand gestures activates this region in chimpanzees (Taglialatela et al. 2008). Thus, it appears that the specialized role of Broca's area in human language might have been built upon a preexisting function of the inferior frontal cortex that is shared with other Old World primates for the planning and recognition of hand and mouth action sequences (Arbib 2005).

A homologue of Broca's area has been cytoarchitectonically identified in all species of great apes (Kreht 1936; Bailey et al. 1950; Sherwood et al. 2003; Schenker et al. 2008) and several Old World monkeys (Watanabe-Sawaguchi et al. 1991; Petrides and Pandya 2001). However, few studies have examined this region's anatomy in a comparative context. Although diffusion tensor imaging has demonstrated that Broca's area in humans maintains greater connections with the middle temporal gyrus than in chimpanzees or macaque monkeys (Rilling et al. 2008), many other open questions remain regarding how this cortical area has changed during human evolution to support language behavior since our lineage branched from a common ancestor with chimpanzees 6–8 million years ago.

One aspect of language representation in the human brain that is particularly striking is its functional lateralization, with 94% of right-handed individuals exhibiting left hemisphere language dominance (Springer et al. 1999). This relationship has led researchers to examine anatomical asymmetries of Broca's area (Falzi et al. 1982; Foundas et al. 1998; Amunts et al. 1999; Uylings et al. 2006). Results from these studies have demonstrated that Broca's area in humans is asymmetric in terms of volume, gray level index, complexity and length of dendritic branches, and neuron size and number (reviewed in Schenker et al. 2007; Keller et al. 2009). Notably, however, variation within individuals (between hemispheres) and among individuals in the volume of areas 44 and 45 is substantial (Amunts et al. 1999, 2003). Moreover, there is extensive variability in the location of areas 44 and 45 relative to sulcal landmarks in both humans (Amunts et al. 1999, 2004) and chimpanzees (Sherwood et al. 2003). Although leftward asymmetry of the inferior frontal gyrus (IFG) has been reported for African great apes based on magnetic resonance imaging (MRI) morphometry (Cantalupo and Hopkins 2001; Hopkins et al. 2008), there are no data published concerning the size or asymmetry of cytoarchitectonically defined areas 44 and 45 in nonhuman primates. In the absence of such comparative data, it remains unclear whether the size of this cortical region has undergone relative expansion during human evolution, as has been claimed for other prefrontal areas (Semendeferi et al. 2001).

To establish a comparative foundation for evaluating the size and asymmetry of Broca's area in humans, we used design-based stereological methods to estimate volume, total neuron number, and neuron density in Brodmann's areas 44 and 45 of chimpanzees (*Pan troglodytes*). The brain specimens in the current study were obtained from chimpanzees with known hand preferences, providing a unique opportunity to examine the interrelationship among behavior, histology, and gross morphology of Broca's area homologue in one of our species' closest living relatives. We analyzed variation in the position of areas 44 and 45 across individuals using probabilistic mapping and in reference to sulcal folding patterns of the IFG. We also investigated whether population-level asymmetry is present in areas 44 and 45 of chimpanzees and tested for correlations between asymmetry of these cortical areas and measures of IFG morphology and hand preference on 2 behavioral tasks. Finally, we compared the difference in volume between Broca's area in humans and chimpanzees relative to other cortical areas, finding that areas 44 and 45 in the left hemisphere show among the greatest volumetric enlargement in humans of any neocortical regions examined to date.

Table 1

Previously published data on handedness (Hopkins 1995; Hopkins and Cantalupo 2004; Taglialatela et al. 2006), asymmetry of the volume of the IFG (Hopkins et al. 2008), and asymmetry of the length of the fronto-orbital sulcus (Hopkins and Cantalupo 2004)

Subjects	Tube task HI	Gesture task HI	Fronto-orbital sulcus length AQ	IFG volume AQ
C0630	1.00	0.58	5.2	−30.0
C0342	0.36	−0.23	−84.8	−31.0
C0406	0.34	−0.17	−39.8	−21.0
C0336	−0.16	1.00	−66.1	−11.7
C0408	1.00	N/A	−22.0	29.0
C0242	0.68	N/A	−17.0	−0.2
C0507	0.91	0.04	−15.8	−40.0
C0491	0.51	0.00	−71.2	58.0
C0423	0.35	0.56	−45.9	−39.0
C0301	−0.71	0.43	−67.1	−12.0
C0273	0.65	0.33	−18.0	−7.3
C0367	−1.00	−0.11	−26.6	−15.0

Note: Positive values indicate a rightward asymmetry. Negative values indicate a leftward asymmetry; N/A, not available.

Methods

Subjects

Twelve chimpanzee subjects were used in this study, including 6 females (mean age at death = 37.8 years, standard deviation [SD] = 12.9, range = 13–48) and 6 males (mean age at death = 29.3 years, SD = 10.8, range = 17–41). Five of the chimpanzee subjects had been wild caught and lived in captivity since their capture. The remaining 7 chimpanzees were born in captivity. All subjects lived in social groups ranging from 2 to 13 individuals at Yerkes National Primate Research Center and were housed according to institutional guidelines. Brains were collected after subjects died from causes unrelated to the current study.

Behavioral Measurements

Handedness data for these subjects have been previously reported (Hopkins 1995; Hopkins and Cantalupo 2004; Taglialatela et al. 2006). To assess handedness, 2 different tasks were used. First, hand preference was observed in response to a task measuring coordinated bimanual actions, referred to as the tube task. For this task, peanut butter was applied to the inside of polyvinylchloride tubes and presented to the subject. Hand use was recorded for each event in which the subjects reached into the tube with their finger, extracted peanut butter, and brought it to their mouth. Hand preference on this task is stable across the lifespan of an individual based on test–retest analyses (Hopkins 2007). Handedness data on the tube task were available for all subjects. In the second task, the subject's hand preference for manual gesturing was recorded. In each trial, the experimenter approached the chimpanzee's home cage carrying food. A piece of food was offered until the chimpanzee produced an open hand begging gesture. Other manual responses (e.g., banging or clapping) were not counted as gestures. The hand used to request food was recorded for each trial. Handedness data on the gesture task were available for 10 of the 12 subjects. A minimum of 30 responses were obtained for each individual for each task. A handedness index (HI) was derived for each subject for each task by subtracting the number of left-handed responses from the number of right-handed responses and dividing the total number of responses: HI = (R − L)/(R + L). Positive values reflect right-hand preference, and negative values represent left-hand preference (Table 1). The absolute value of the HI corresponds to the consistency of directional hand preference. Subjects with z scores greater than 1.95 or less than −1.95 were classified as right- and left-handed, respectively. Subjects with z scores between −1.95 and 1.95 were classified as having no preference. Neuroanatomical measurements were performed blind to the HI scores of the subjects.

MRI Collection

Within 14 h of each subject's death, the brain was removed and immersed in 10% formalin at necropsy. MRI scans of the postmortem brain specimens were acquired on a commercial 1.5 T GE high-gradient MRI scanner equipped with 8.3 software (GE Medical Systems, Milwaukee, WI). Coronal T_1-weighted MR images were acquired through the entire brain with time repetition = 666.7 ms and time echo = 14.5 ms with an echo train of 2. Slices were obtained as 1.5-mm-thick contiguous sections with a matrix size of 256 × 256 and a field of view of 16.0 × 16.0 cm, resulting in a final voxel size of 0.625 × 0.625 × 1.5 mm.

Tissue Preparation and Staining

The frontal lobe was blocked from each brain with a coronal cut at the level of the precentral gyrus. Tissue blocks were cryoprotected by immersion in buffered sucrose solutions up to 30%, embedded in tissue medium, frozen in a slur of dry ice and isopentane, and sectioned at 40 μm with a sliding microtome in the coronal plane. Every 10th section (400 μm apart) was stained for Nissl substance with a solution of 0.5% cresyl violet to visualize cytoarchitecture. Every 20th section was stained for myelin using the Gallyas (1971) method.

Immunohistochemistry for nonphosphorylated neurofilament protein was also performed on a 1:20 series of sections. Free-floating sections were stained with mouse monoclonal antibodies to non-phosphorylated epitopes on the neurofilament protein triplet (SMI-32 antibody; Covance International, The Netherlands; dilution 1:3000). Prior to immunostaining, sections were rinsed thoroughly in phosphate-buffered saline (PBS) and pretreated for antigen retrieval by incubation in 10 mM sodium citrate buffer (pH 8.5) at 85 °C in a water bath. Sections were then immersed in a solution of 0.75% hydrogen peroxide in 75% methanol to eliminate endogenous peroxidase activity. After additional rinsing, sections were incubated in the primary antibody for 48 h on a rotating table at 4 °C in a diluent containing PBS with 4% normal horse serum, 1% bovine serum albumin, 0.1% Triton X-100, and 3% dry milk. After rinsing in PBS, sections were incubated in the secondary antibody (biotinylated antimouse IgG, Vector Laboratories, Burlingame, CA; dilution 1:200) and processed with the avidin–biotin–peroxidase method using a Vectastain Elite ABC kit (Vector Laboratories). Immunoreactivity was revealed using a modified glucose oxidase-3,3′-diaminobenzidine-nickel intensification method (Shu et al. 1988; Van der Gucht et al. 2006). Every other section was counterstained with cresyl violet to visualize nonimmunoreactive neurons and cytoarchitectonic boundaries. Specificity of the

reaction was confirmed by processing negative control sections as described but excluding the primary antibody. No immunostaining was observed in control sections.

Area Identification

In both hemispheres, the boundaries of Brodmann's areas 44 and 45 were manually drawn in serial sections with the StereoInvestigator software (MBF Bioscience, Williston, VT) using a 2.5× objective (N.A. 0.075) on a Zeiss Axioplan 2 microscope (Fig. 1). Regions of interest were identified using criteria from previous descriptions (Bailey et al. 1950; Sherwood et al. 2003; Schenker et al. 2008). Adjacent areas were differentiated from areas 44 and 45 on the basis of cytoarchitectonic criteria (Fig. 2). In brief, posterior to area 44, the overall thickness of the cortex is greater, layer IV is poorly defined, and neurons in layer III are not markedly larger than those in layer V. More dorsally, layer III neurons are smaller and not as large as those in layer V, whereas layer IV is similar in width to area 44. Anterior and dorsal to areas 44 and 45, layer IV becomes more visible, whereas neurons in layer V become smaller. Anterior to area 45, layer II becomes narrow and dense and layer IV is more prominent, whereas the overall thickness of cortex is decreased. Ventral to areas 44 and 45, the cortex is quite narrow and layers II and IV are prominent.

A key cytoarchitectural characteristic of areas 44 and 45 is the presence of large pyramidal neurons in lower layer III that are often larger than those in layer V. Also layers III and V are separated by

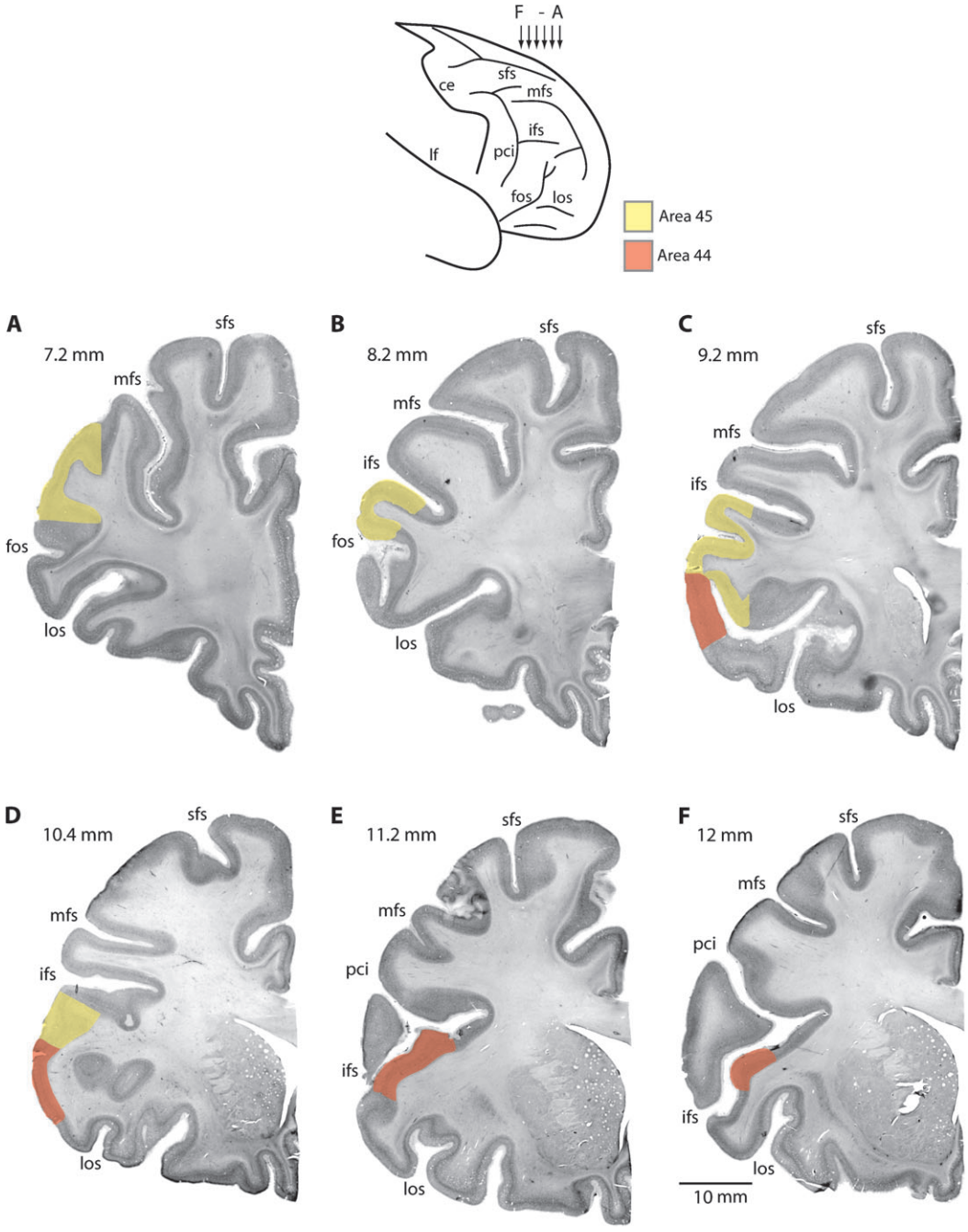

Figure 1. An anterior (*A*; 7.2 mm from the frontal pole) to posterior (*F*; 12 mm from the frontal pole) coronal series of a chimpanzee right hemisphere (C0423) stained for Nissl substance showing the region that contains areas 44 and 45. Abbreviations: ce = central fissure; fos = fronto-orbital sulcus; ifs = inferior frontal sulcus; lf = lateral fissure; los = lateral orbital sulcus; mfs = middle frontal sulcus; pci = inferior precentral sulcus; and sfs = superior frontal sulcus. Scale bar = 10 mm.

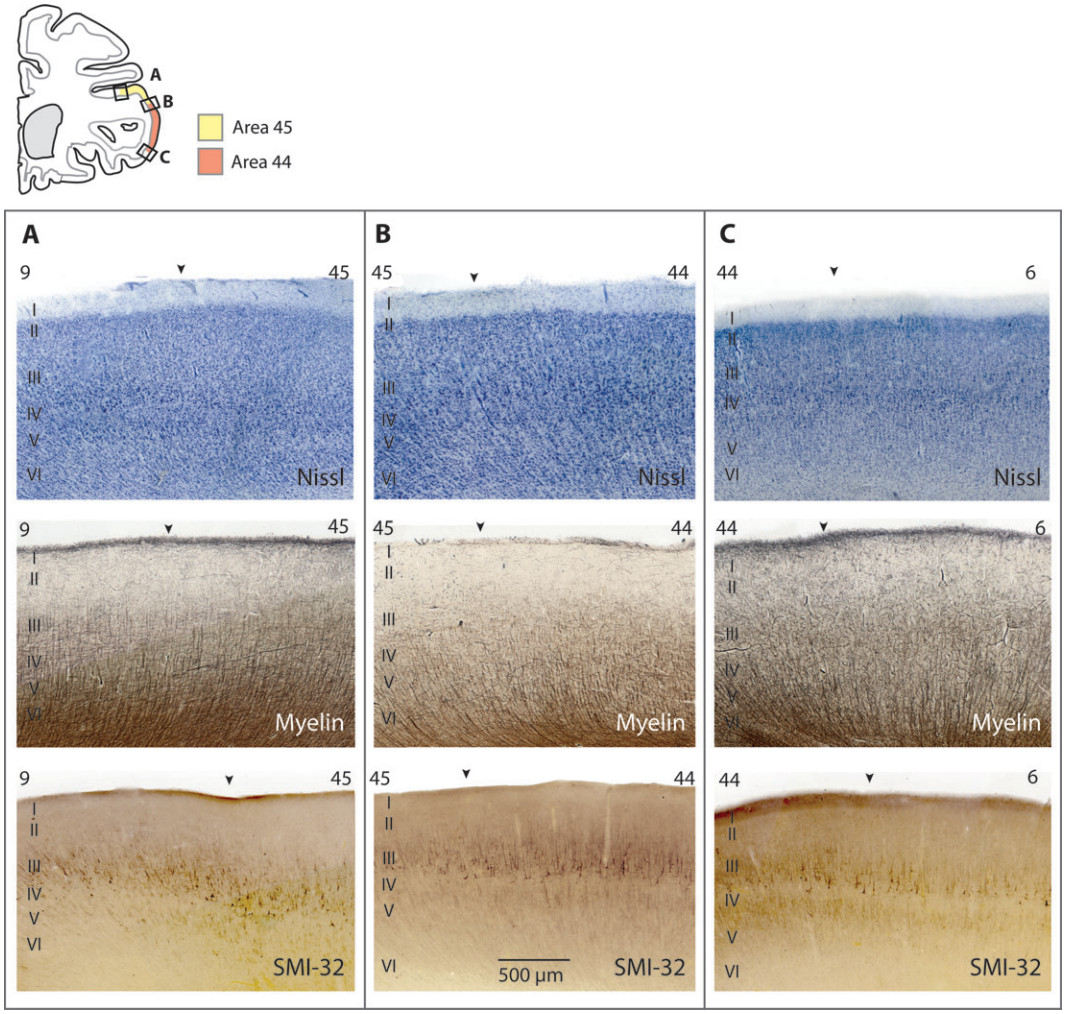

Figure 2. Representative photomicrographs of the cortex of the IFG in a chimpanzee (C0491), illustrating the right hemisphere sectioned in the coronal plane and stained for Nissl substance, myelin, and nonphosporylated neurofilament protein. Arrows indicate the boundaries between areas. Scale bar = 500 μm.

a narrow dysgranular layer IV in area 44 that widens in area 45. In sections immunostained for nonphosphorylated neurofilament protein with the SMI-32 antibody, large pyramidal neurons at the bottom of layer III are particularly conspicuous and aid in delineation of areas 44 and 45 from surrounding cortical areas. The myeloarchitecture is also useful in distinguishing between areas 44 and 45, with more horizontal myelinated fibers present in upper portions of layer III in area 45 than in area 44 (Fig. 2).

Probabilistic Mapping

The exact boundaries of each cortical area, as observed under the microscope, were drawn on printouts of images produced from digital flatbed scans of the histological slides (Fig. 1). The cortical area boundaries were then manually delineated on MRI scans of the brains, which had been collected prior to sectioning. Each brain was reoriented to match the plane of sectioning using prominent landmarks on each of the histological sections to the morphology of the MRI slices in order to facilitate the transfer of boundaries from the histological slides to the MRIs. Object maps were created using Analyze 7.0 software (AnalyzeDirect, Overland Park, KS) for each cortical area by manually drawing its extent on every MRI slice in which it occurred.

After object maps of each cortical area were transferred to the MRI scans, the 3D image of each brain was coregistered to a template chimpanzee brain (for details about the creation of the template, see Rilling et al. 2007). Each individual MRI scan was oriented using the AC–PC line and then coregistered to the template using 3-dimensional nonrigid registration (Analyze 7.0). The locations of the cortical areas were integrated across all subjects on a voxel-by-voxel basis. The resulting probability map indicates the regions of overlap across all subjects as projected onto the template brain.

Measurements of Total Neocortical Gray Matter

The total volume of neocortical gray matter was estimated for each hemisphere. The boundary of neocortical gray matter (excluding the amygdala and hippocampus) was manually traced using ImageJ 1.38× (National Institutes of Health, Bethesda, MD) on a systematic random sample of 10 coronal sections from each hemisphere of the MRIs. The areas of the bounded cortex in each section were calculated, summed, and multiplied by the distance between sections to estimate the volume.

Shrinkage Correction

We calculated correction factors for each individual tissue block to adjust volumes for variation in the shrinkage that occurs during histological processing. For most blocks, a presectioning mass was available. These presectioning masses were converted to volume by dividing the specific gravity for brain tissue (1.036 g/cc; Gompertz 1902). For blocks without presectioning masses available, presectioning volumes were estimated by outlining the extent of the block on postmortem MRI scans using Analyze 7.0 software. Postprocessing volumes were estimated using digitally scanned images of each Nissl-stained series. The outline of each section was determined by

thresholding using ImageJ software, and the area for each section was calculated. The summed area of sections was converted to volume by multiplying by the distance between measured sections (i.e., for a 1:10 series of 40-μm-thick sections, the distance between sections is 400 μm). To obtain a correction factor unique to each block, the presectioning block volume was divided by the postprocessing volume. The shrinkage correction factor, which represents the fold difference between presectioning and postprocessing volume, averaged 2.88 ± 0.73 (±SD).

Cortical Area Volumes

Volumetric data were collected from Nissl-stained histological sections for each cortical area with the Cavalieri method (Gundersen et al. 1988), using a 500-μm point counting grid in the StereoInvestigator software. In each hemisphere, 6–16 sections were analyzed at intervals of 400 or 800 μm between sections for each cortical area. As required by the Cavalieri method, sampled sections from each specimen were chosen at standard intervals for each area and the starting section was picked randomly from the first interval. The coefficient of error (Gundersen et al. 1999; $m = 1$) was less than 0.036 for each cortical area in each specimen (Table 2); such low values indicate that the precision of the volume estimates was high and that the sampling parameters were sufficient. Each cortical area's volume was multiplied by the appropriate shrinkage correction factor to obtain a value representing the presectioning volume.

Neuron Counts

To estimate total neuron numbers in Nissl-stained sections, we used the optical fractionator method (West et al. 1991) with a 50 × 50-μm counting frame and a 1200 × 1200-μm scan grid on the same sections used for volumetric estimates. We used a standard disector depth of 7 μm in the specimens, with a 3-μm guard zone at the top. Section thickness was measured at every fifth site during counting. Neurons were counted in layers II–VI only if a clear nucleolus came into focus within the permitted boundaries of the counting frame, according to the principles of the optical fractionator method (West et al. 1991). The calculated coefficients of error (Schmitz and Hof 2000) were within the range of ≤0.10 for each cortical area in each specimen (Table 3). Neuron density was calculated as the ratio of total neuron number over the shrinkage-corrected cortical area volume for each region of interest.

Fronto-Orbital Sulcus Length

The fronto-orbital sulcus is a prominent landmark in the opercular portion of the IFG. The length of the sulcus was traced on every parasagittal (1 mm thick) MRI slice in which it appeared from the first lateral slice in which it was present to the slice just preceding the opening of the insula (Table 1; Hopkins and Cantalupo 2004). This measurement estimates the surface area bounded by the fronto-orbital sulcus.

IFG Volume

Estimation of the volume of the IFG was performed in the axial plane. The posterior and anterior borders of the IFG were the inferior precentral sulcus and the fronto-orbital sulcus, respectively. The entire gyrus between these sulci, including both gray and white matter, was traced with the surface of the brain serving as the lateral border and the medial ends of the sulci serving as the medial borders. The area was traced on every MRI slice (1 mm thick) on which both the inferior precentral sulcus and the fronto-orbital sulcus were present. Area measures were summed across all slices to estimate a volume of the IFG for each hemisphere (Table 1; Hopkins et al. 2008).

Data Analysis

Tables 2 and 3 display volume estimates, total neuron counts, and neuron densities for each cortical area in both the right and left hemispheres. To examine lateralization, an asymmetry quotient (AQ) was calculated using the equation $|(R - L)/[(R + L)/2]|$. Positive values indicate a right greater than left asymmetry, and negative values indicate a left greater than right asymmetry. Population-level asymmetry in each parameter was examined using a Wilcoxon signed-ranks test to determine whether the mean of the AQ was significantly different from zero.

Nonparametric Spearman rank order correlations were calculated between volumes of areas 44 and 45 and neocortical gray matter volume. Correlations were also calculated between AQs for areas 44 and 45 and indices of handedness and between the AQ measures for the length of fronto-orbital sulcus and the volume of the IFG. Age was also tested for an effect on all variables; no effect was observed.

All statistical tests were conducted using JMP IN 4.02 statistical software (SAS Institute, 2000, Cary, NC). Statistical significance was considered at $\alpha = 0.05$. Sequential Bonferroni corrections of α were made on a per-hypothesis basis.

Validation and Interobserver Variability

The inherent subjectivity in defining cytoarchitectonic boundaries and the challenges associated with transferring cortical area borders from histological slides back onto MRI scans makes an evaluation of intra- and interobserver variability an important component to the validation of these methods. Five specimens were randomly selected for comparison, and the cytoarchitectonic borders of each cortical area were independently delineated by a second observer (M.A.S) blind to the results of the first (N.M.S). The volume of each cortical area was

Table 2
Stereological estimates and CE of shrinkage-corrected volumes (mm^3) for each cortical area

						Volume (mm^3)							
Subject	Sex	Age	Whole brain (cm^3)	Left neocortical gray (cm^3)	Right neocortical gray (cm^3)	Left 44	CE	Left 45	CE	Right 44	CE	Right 45	CE
C0630	Female	13	415.4	96.5	97.9	669.1	0.026	746.4	0.018	760.0	0.019	801.2	0.012
C0342	Female	35	348.1	91.0	93.8	437.8	0.008	413.0	0.013	568.5	0.006	468.1	0.009
C0406	Female	42	327.8	75.6	77.0	650.5	0.011	768.0	0.013	788.1	0.018	523.3	0.014
C0336	Female	44	332.9	81.9	81.2	594.1	0.011	326.6	0.036	1013.0	0.008	1049.8	0.013
C0408	Female	45	312.9	85.4	83.3	563.7	0.010	329.3	0.010	554.0	0.011	445.8	0.010
C0242	Female	48	298.2	75.0	77.0	547.9	0.020	311.8	0.036	831.0	0.006	706.5	0.009
C0507	Male	17	384.0	102.9	98.0	963.9	0.011	757.2	0.008	639.1	0.017	735.7	0.018
C0491	Male	18	364.6	84.7	88.2	204.6	0.010	271.4	0.013	803.6	0.005	562.0	0.007
C0423	Male	25	419.7	96.8	96.1	557.1	0.018	684.8	0.012	501.3	0.010	483.8	0.012
C0301	Male	35	409.3	104.7	102.9	650.7	0.023	569.6	0.023	400.9	0.028	932.6	0.024
C0273	Male	40	341.2	79.1	76.3	593.1	0.011	291.4	0.015	395.6	0.012	382.9	0.020
C0367	Male	41	377.2	86.8	80.5	778.4	0.036	537.4	0.021	521.1	0.013	506.3	0.025
Mean			360.9	88.4	87.7	600.9		500.6		648.0		633.2	
SD			40.7	10.1	9.6	181.6		199.3		190.9		210.6	
CV			11.3%	11.4%	11.0%	30.2%		39.8%		29.5%		33.3%	

Note: SD, standard deviation; CE, coefficients of error; CV, coefficient of variation.

Table 3
Stereological estimates and CE of neuron density (1000s/mm^3) and total neuron number for each cortical area

	Neuron density (1000s/mm^3)				Total neuron number ($\times 10^6$)							
Subject	Left 44	Left 45	Right 44	Right 45	Left 44	CE	Left 45	CE	Right 44	CE	Right 45	CE
C0630	16.9	16.6	15.3	14.4	11.3	0.07	12.4	0.06	11.6	0.07	11.5	0.06
C0342	13.7	16.7	16.0	15.2	6.0	0.08	6.9	0.08	9.1	0.06	7.1	0.06
C0406	16.0	18.2	19.0	20.8	10.4	0.07	14.0	0.06	15.0	0.07	10.9	0.06
C0336	25.1	23.9	11.1	11.9	14.9	0.06	7.8	0.08	11.2	0.07	12.5	0.06
C0408	17.9	20.0	12.5	16.4	10.1	0.06	6.6	0.07	6.9	0.05	7.3	0.06
C0242	13.1	11.5	17.6	14.6	7.2	0.09	3.6	0.10	14.6	0.07	10.3	0.08
C0507	14.7	14.9	11.1	9.7	14.2	0.06	11.3	0.06	7.1	0.06	7.1	0.06
C0491	15.2	18.8	17.7	18.7	3.1	0.06	5.1	0.07	14.2	0.05	10.5	0.06
C0423	12.9	19.1	15.6	18.6	7.2	0.09	13.1	0.06	7.8	0.05	9.0	0.05
C0301	11.4	11.8	18.7	11.9	7.4	0.07	6.7	0.07	7.5	0.08	11.1	0.06
C0273	17.7	16.8	15.4	18.3	10.5	0.08	4.9	0.09	6.1	0.08	7.0	0.08
C0367	21.7	23.3	16.5	22.5	16.9	0.10	12.5	0.08	8.6	0.08	11.4	0.08
Mean	16.4	17.6	15.5	16.1	9.9		8.7		10.0		9.6	
SD	3.9	3.8	2.7	3.9	4.0		3.7		3.2		2.0	
CV	23.9%	21.8%	17.5%	24.1%	40.4%		42.0%		32.4%		20.9%	

Note: SD, standard deviation; CV, coefficient of variation; CE, coefficients of error.

calculated according to the methods described above, and they were subsequently mapped onto the accompanying MRIs.

To assess the impact of interobserver variability on both the absolute volume and the AQs, the intraclass correlation coefficient (ICC) was calculated between measurements of each cortical area by each observer. These results indicate a strong agreement between observers for both the absolute volume (ICC = 0.91; $P < 0.001$) and the AQ (ICC = 0.93; $P < 0.0001$). Thus, the subjective judgment of area boundaries by these 2 observers covaries in a systematic fashion, suggesting that the quantitative measures of regional volumes and neuron numbers presented here are reliable.

Another area of potential variability was the transfer of area boundaries onto the associated MRIs. Analysis of the correlation between histologically derived volumes and the volumes mapped onto MRIs revealed excellent congruency ($r = 0.97$; $P < 0.001$). Area volumes mapped onto the MRIs were on average 15% lower than estimates of volumes obtained directly from the histological sections.

Finally, when each cortical area was mapped back onto the MRIs and the percentage of spatial overlap between the volumes delineated by Observer 1 and Observer 2 was calculated, a mean percentage overlap of 65 ± 10% (SD) was obtained. Thus, a portion of interindividual variation in the location of cortical areas can be attributed to differences among observers in the subjective definition of boundaries. Therefore, our probability maps should cautiously be considered underestimates. Nonetheless, it is notable that our findings regarding interindividual variation in stereological measures and the spatial position of cortical areas are very similar to previous results from humans based on the "observer-independent" gray level index method of area boundary identification (Amunts et al. 1999; Uylings et al. 2006).

Results

Probabilistic Mapping

Figure 3 shows the location of areas 44 and 45 rendered on the reconstructed cortical surface for each individual. Areas 44 and 45 were both found in the IFG, often extending into the inferior frontal and fronto-orbital sulci. Area 44 was most often located immediately anterior to, and sometimes within (in 20 of 24 hemispheres), the inferior precentral sulcus. Area 45 was most typically located anterior to the fronto-orbital sulcus and sometimes superior to area 44. Despite this general consistency, there was extensive interindividual variation in the precise boundaries of these cortical areas relative to the position of sulcal features.

Figure 4 shows probabilistic maps of areas 44 and 45 registered to a template chimpanzee brain. On average, both regions were located ventral to the inferior frontal sulcus in the template coordinate space. However, areas 44 and 45 displayed considerable interindividual variability in their positions on the template and exhibited limited overlapped among the 12 subjects. To estimate the extent of spatial congruence of each cortical area across individuals, we calculated the volume where at least 5 of 12 subjects showed overlap. These volumes and centroid coordinates are presented in Table 4.

Stereological Data

The volumes, neuron numbers, and neuron densities from areas 44 and 45 also displayed a high degree of variability among individuals (Fig. 5). Coefficients of variation ranged from 29.5% to 39.8% for volume, 22.9% to 25.1% for neuron density, and 20.9% to 42.0% for total neuron number (Tables 2 and 3). This variation is at least twice that for whole brain volume (11.3%) and the volume of neocortical gray matter in each hemisphere (11.0–11.4%). We analyzed stereological data using mixed-model analyses of variance (ANOVAs) with sex as a between-subjects factor and hemisphere and area as within-subjects factors. No significant effects or interactions were observed (Fig. 5).

We hypothesized that the volume of areas 44 and 45 within an individual would covary with the volume of the neocortical gray matter. To test this prediction, we calculated a correlation matrix among the volumes of area 44, area 45, and neocortical gray matter. However, the volumes of areas 44 and 45 were not significantly correlated with neocortical gray matter volume in the hemisphere of their location (left 44: $r_s = 0.39$, $P = 0.21$; left 45: $r_s = 0.50$, $P = 0.10$; right 44: $r_s = -0.17$, $P = 0.60$; right 45: $r_s = 0.43$, $P = 0.17$). The volumes of areas 44 and 45 in the left hemisphere were correlated with each other prior to Bonferroni correction but not after ($r_s = 0.65$, $P = 0.02$, $P' = 0.13$). The volumes of areas 44 and 45 in the right hemisphere were not significantly correlated ($r_s = 0.52$, $P = 0.08$).

Asymmetry

We examined all stereological data for evidence of population-level asymmetry by using a Wilcoxon signed-ranks test to determine whether the distribution of AQs differed significantly from zero (i.e., symmetry). Although there was notable asymmetry in certain individuals (e.g., 8 of 12 individuals had greater than 10% asymmetry in total neuron number in area 44, area 45, or both; 7 of 12 had greater than 10% asymmetry in volume in one or both areas), we found no evidence of a consistent directional asymmetry at the population level for any of the stereological measures (Table 5).

Correlations with Handedness

In humans, individuals with greater right-hand preference are more likely to display left hemisphere language dominance (Knecht et al. 2000). Furthermore, data from structural MRI suggest that hemispheric language dominance is related to asymmetries of the IFG in humans (Foundas et al. 1996). Prompted by these results, we tested for correlations between the degree of asymmetry in stereological measures and handedness on a bimanual coordinated task and a communicative gesturing task. However, no significant correlations were found between asymmetry of areas 44 and 45 and either

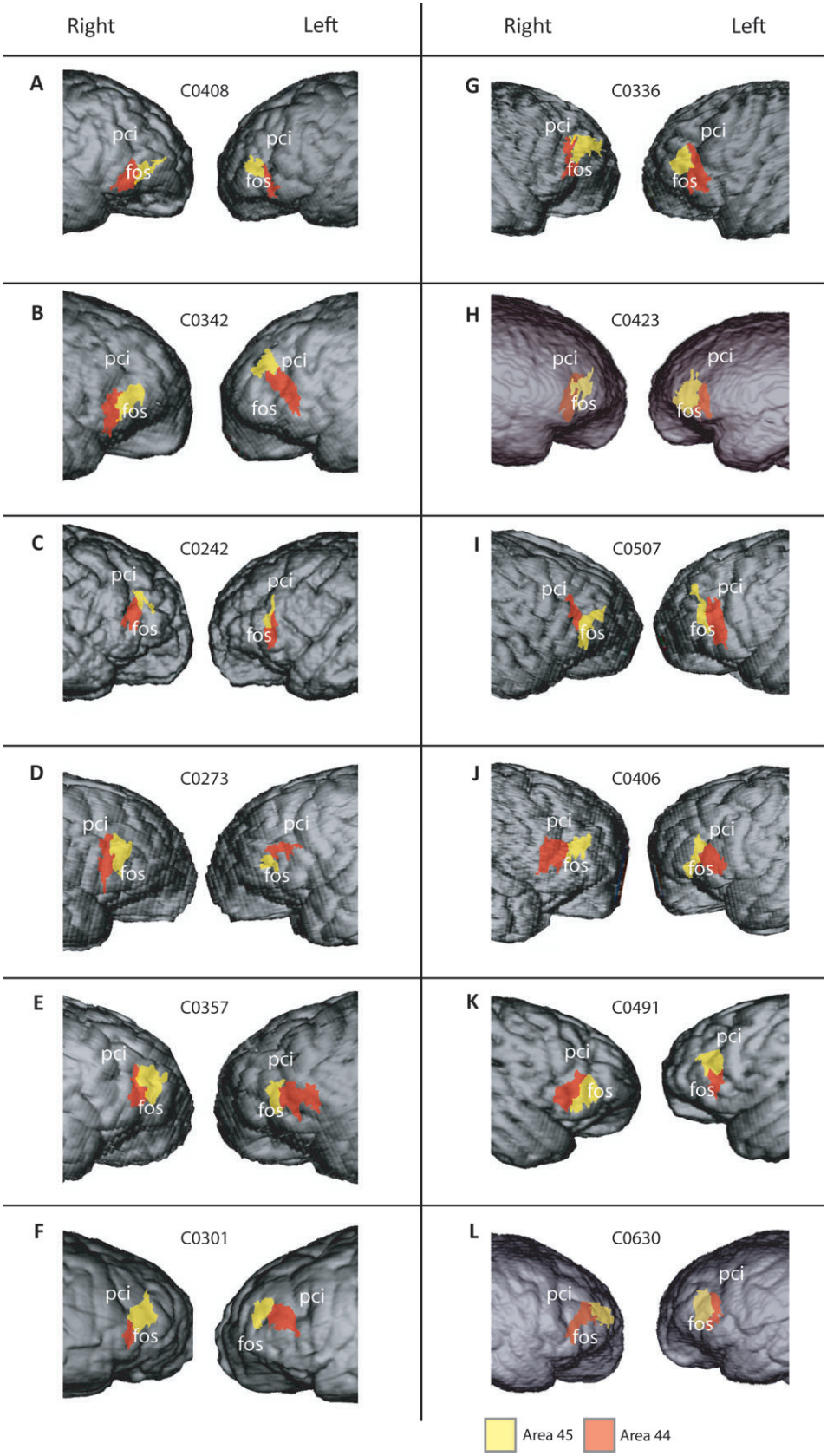

Figure 3. Reconstructed lateral views of the magnetic resonance images of both hemispheres in 12 chimpanzees. The extent of areas 44 and 45 on the lateral surface of the brain are shown in red and yellow, respectively. The position of areas 44 and 45 where they lie within sulci is not visible (*A*: C0408, *B*: C0342, *C*: C0242, *D*: C0273, *E*: C0357, *F*: C0301, *G*: C0336, *H*: C0423, *I*: C0507, *J*: C0406, *K*: C0491, and *L*: C0630). Abbreviations: fos = fronto-orbital sulcus; pci = inferior precentral sulcus.

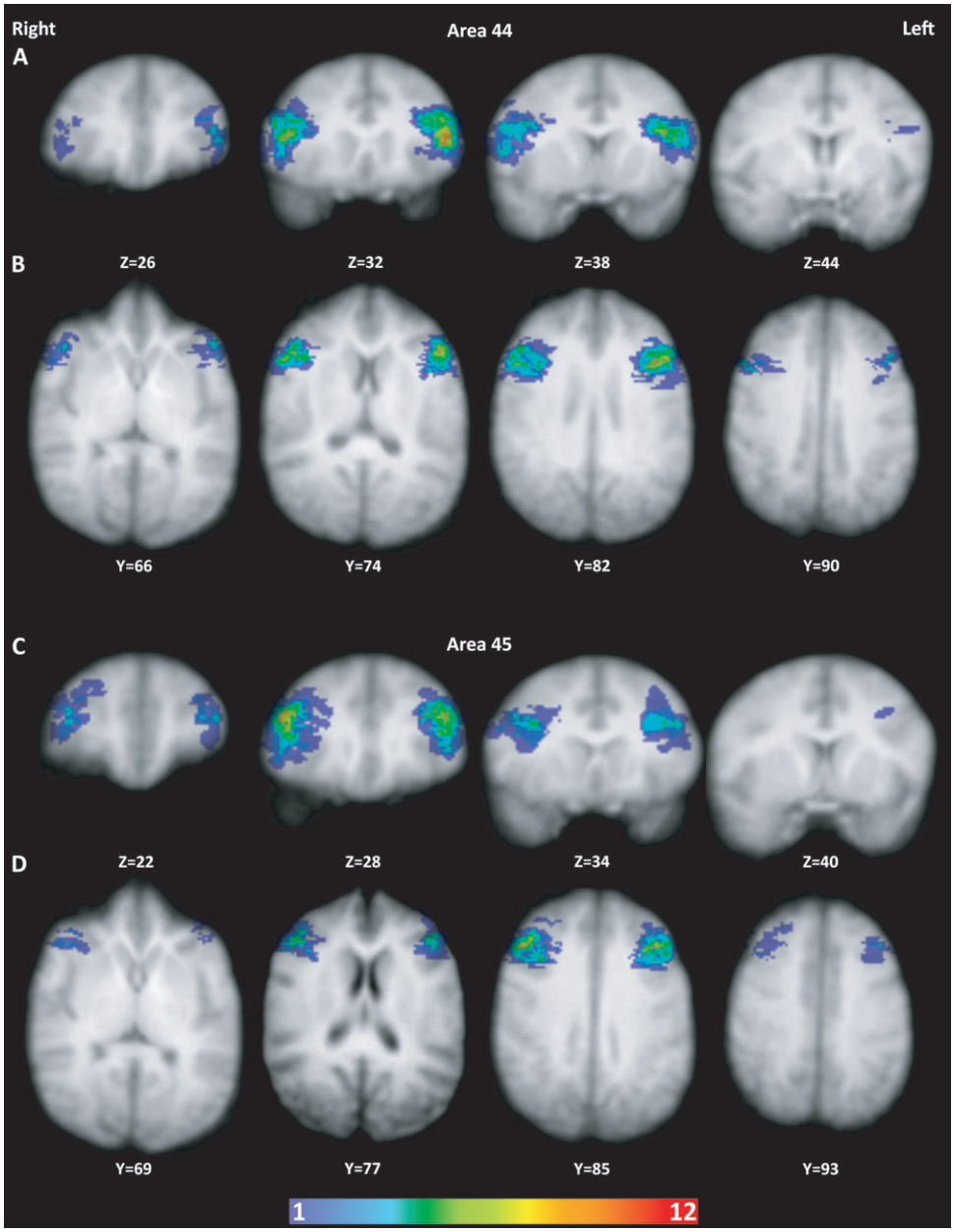

Figure 4. Probability maps of the location of areas 44 and 45 on a template chimpanzee brain. Coronal and axial series through area 44 (*A*, *B*) and area 45 (*C*, *D*) are shown with coordinates indicating the level of the sections. Colors indicate the number of individuals in which the area is occupied by the region of interest. Warmer colors (more red) indicate greater numbers of individuals overlapping, and cooler colors indicate fewer numbers of individuals overlapping.

Table 4
Volumes and centroid *x*, *y*, and *z* coordinates for the regions of areas 44 and 45 that overlap in at least 5 of 12 individuals

			Centroid		
Area	Hemisphere	Volume (mm^3)	*x*	*y*	*z*
Area 44	Left	642	94	79	34
	Right	349	35	78	33
Area 45	Left	280	91	83	29
	Right	249	38	83	27

HI in these individuals (Table 6). Furthermore, there were no significant relationships between AQs, hand preference category (right or nonright handed), or sex using 2-way ANOVA.

Correlations with Fronto-Orbital Sulcus Length and IFG Volume

Previous studies have reported population-level asymmetry in various morphological measurements of the inferior frontal region in chimpanzees based on MRI (Cantalupo and Hopkins 2001; Hopkins and Cantalupo 2004). To explore the underlying basis of these asymmetries in chimpanzees, we tested the relationship between the AQs of stereological data and morphological measures of the IFG by calculating nonparametric Spearman's rho correlations. We found that asymmetry in the volume of the IFG was significantly positively correlated with asymmetry of the total number of neurons in area 45 ($r_s = 0.83$, $P' < 0.001$) and asymmetry of the volume of area 45 prior to Bonferroni correction ($r_s = 0.64$, $P = 0.03$, $P' = 0.08$). However, no significant

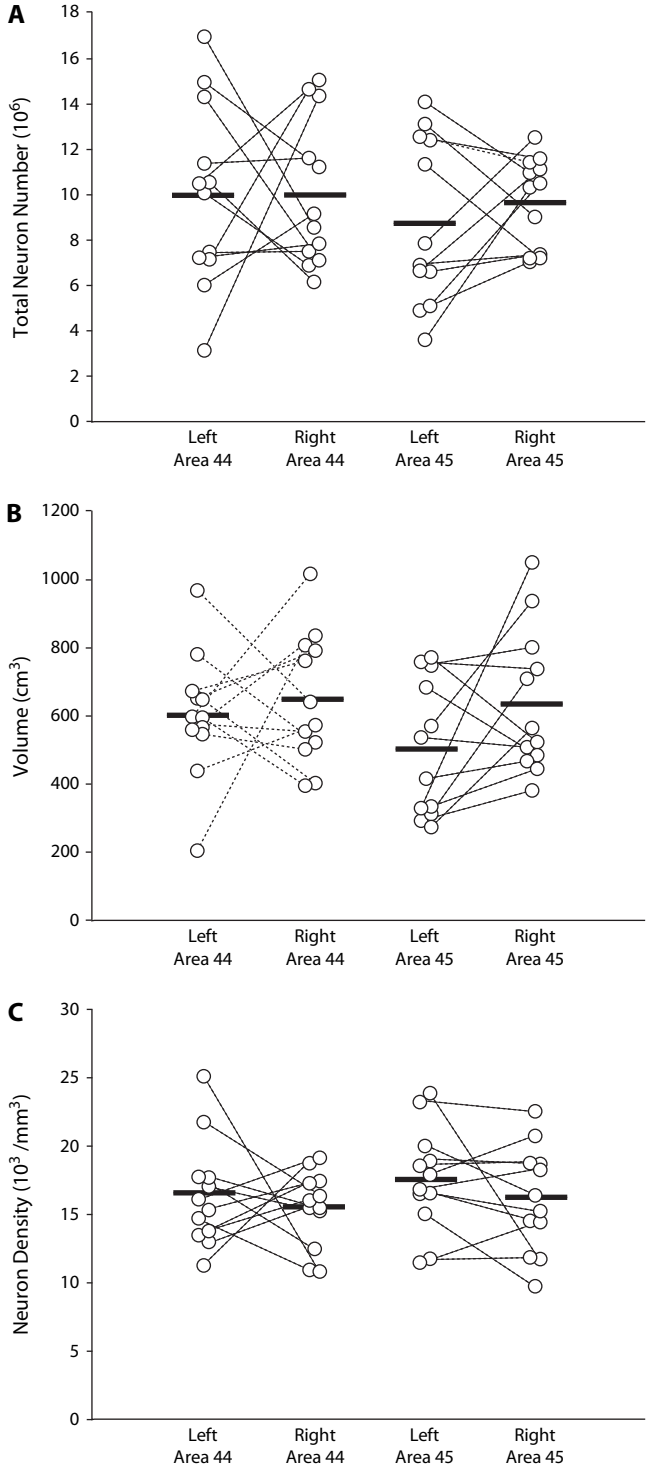

Figure 5. Total neuron number (*A*), cortical area volume (*B*), and neuron density (*C*) are plotted by region of interest. Bars indicate the mean values for each parameter in each region. Dotted lines connect the left and right hemisphere values within an individual.

correlations were found between asymmetry in the length of the fronto-orbital sulcus and AQs of stereological data.

Discussion

We investigated the interrelationship among behavior, histology, and gross morphology of Broca's area homologue in chimpanzees. Untangling the interaction between the structure and function of this cortical area in chimpanzees provides a crucial comparative foundation for determining which characteristics of Broca's area in humans are inherited from our common ancestry with great apes and which are more recent specializations added during evolution and might support linguistic processing.

There is substantial variation in the precise location and topographic extent of Broca's area in humans, both among individuals and between hemispheres within the same individual (Amunts et al. 1999, 2004). Previous examination of chimpanzees also indicated variability in the location of Broca's area homologue in chimpanzees (Sherwood et al. 2003). Here, we have further documented variation in the size and location of areas 44 and 45 in chimpanzees, obtaining results that are consistent with previous quantitative data from these cortical areas in humans (Amunts et al. 1999; Uylings et al. 2006). Specifically, probability maps for humans showed very little overlap in the location of areas 44 and 45 among individuals when registered to a common template brain coordinate space (Amunts et al. 1999). Similarly, our data showed that chimpanzee brains are also highly variable in the location of these cytoarchitectonic areas within the inferior frontal cortex. The maximum degree of cortical area overlap in the template chimpanzee brain was observed from 10 of 12 individuals for area 44 in the left hemisphere and occupied only 2 mm^3. These results are congruent with the large amount of variation in the pattern of sulcal anatomy in the IFG of humans and chimpanzees (Connolly 1950; Ono et al. 1990; Duvernoy 1991; Fischl et al. 2007; Keller et al. 2007). Despite this variation among brains, however, there was a certain degree of consistency in the location of the cytoarchitectural boundaries of areas 44 and 45 in respect to the position of sulci. In particular, Broca's area was usually found anterior to the inferior precentral sulcus and ventral to the inferior frontal sulcus in chimpanzees, although rare exceptions were noted. Thus, we conclude that although it might be possible to use sulcal patterns on MRIs and endocasts to determine the general location of Broca's area, it is problematic to use these gross anatomical landmarks to define the position of its constituent cytoarchitectonic areas without further histological confirmation.

Table 5
Results of Wilcoxon signed-ranks tests for population-level asymmetry

	Total neuron number		Volume		Neuron density	
	Z	*P*	*Z*	*P*	*Z*	*P*
Area 44	0.165	0.87	0.078	0.94	0.553	0.59
Area 45	1.219	0.25	1.177	0.24	1.320	0.21

Table 6
Results of Spearman's rho correlations between stereological parameters and HI on a bimanual coordination task and on a manual gesture task

	Tube task		Gesture task	
Parameter	r_s	*P*	r_s	*P*
Neuron number AQ 44	0.22	0.48	−0.15	0.68
Neuron number AQ 45	−0.04	0.90	0.08	0.83
Volume AQ 44	0.35	0.27	0.10	0.78
Volume AQ 45	−0.16	0.62	−0.03	0.93
Neuron density AQ 44	−0.22	0.48	−0.19	0.60
Neuron density AQ 45	−0.19	0.56	−0.37	0.29

Recently, an increasing number of studies have begun investigating the brains of chimpanzees using functional imaging techniques, such as positron emission tomography (Rilling et al. 2007; Hopkins et al. 2008; Taglialatela et al. 2008, 2009; Parr et al. 2009). Such studies of our close phylogenetic relatives are crucial for understanding how human brain function may be distinctive. In most of these neuroimaging studies, interpretations of activation have been guided by reference to the classic map of the chimpanzee neocortex by Bailey et al. (1950). That cortical map is limited, however, because it was based on a relatively small sample size and it does not incorporate information about individual variability. The data from the present study provide coordinates on a template chimpanzee brain that localize Brodmann's areas 44 and 45 based on cytoarchitectural criteria. Similar probability maps of areas 44 and 45 in humans, for example, have been combined with functional imaging data to segment the contribution of each component of Broca's area to task-specific verbal fluency and semantic retrieval (Amunts et al. 2004; Heim et al. 2008). Probability maps of areas 44 and 45 in chimpanzees will allow researchers to investigate more precisely the functional activation of these cortical areas in our closest living relatives, representing a crucial step in developing more comprehensive studies to examine the evolutionary precursors to the human capacity for language.

Our stereological findings demonstrated considerable variation in Brodmann's areas 44 and 45 of chimpanzees in terms of total neuron number, neuron density, and regional volume. The variation in total neuron number and volume in the current sample is comparable to that reported for Broca's area in humans (Fig. 6; Uylings et al. 2006). In both chimpanzees and humans, variation in the size of these cortical areas exceeds that for total brain size (human brain volume CV = 15.5%, see Amunts et al. [1999] and Uylings et al. [2006]; chimpanzee brain volume CV = 11.3%). Moreover, we did not find a correlation between the size of Broca's area in chimpanzee and neocortical gray matter volume. Taken together, these results suggest that certain factors may influence the size of these higher order cytoarchitectonic areas independently of the neocortex as a whole. Notably, this contrasts with findings showing that the size of primary sensory areas (S1, A1, and V1) covaries significantly with the size of the neocortex in adult short-tailed opossums (Karlen and Krubitzer 2006). Hence, cortical areas that occur earlier in the processing stream might be more tightly constrained in size than those occurring later. Thus, it is conceivable that variation in the size and asymmetry of areas 44 and 45 are related to functional differences among individuals. This possibility has not been previously examined in humans because the brains that were studied by Amunts et al. (1999) and Uylings et al. (2006) lacked behavioral records. However, based on MRI morphometry in a large sample of 56 chimpanzees, handedness for manual gesturing, but not a bimanual coordinated task, was found to be associated with asymmetry of IFG volume (Taglialatela et al. 2006). Our stereological measurements of areas 44 and 45 from the current study did not reveal any such correlations with hand preferences. Because the IFG volume measurement from Taglialatela et al. (2006) combined both gray matter and white matter, it will be worth exploring whether asymmetries in axonal volume and composition are related more directly to measures of behavioral lateralization.

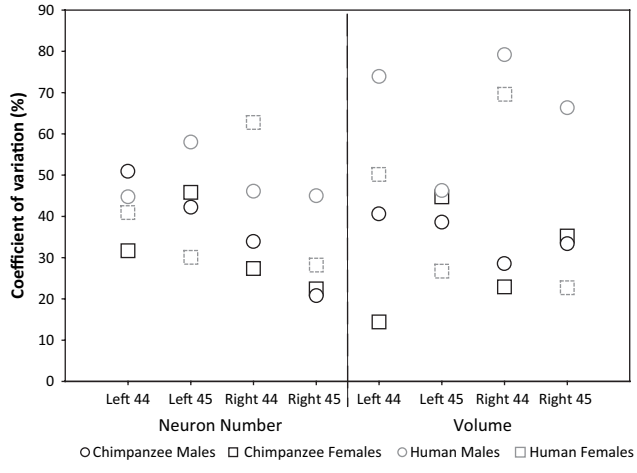

Figure 6. Coefficients of variation for neuron number and volume data from areas 44 and 45 in chimpanzees (black) and humans (gray; Uylings et al. 2006) are plotted by sex (males circles; females squares) for all regions of interest. Note that the level of variation is similar in both species.

It is also possible that asymmetries in areas 44 and 45 are associated with behavioral lateralization outside of the domain of handedness, such as orofacial asymmetries during communicative actions. Experiments in macaque monkeys have shown that stimulation of Broca's area homologue elicits orofacial movements (Petrides et al. 2005). Furthermore, behavioral studies in marmosets, rhesus monkeys, and chimpanzees have shown population-level orofacial asymmetries associated with the production of species-specific vocalizations (Hauser and Marler 1993; Hook-Costigan and Rogers 1998; Fernández-Carriba et al. 2002). More recently, Losin et al. (2008) found a rightward orofacial asymmetry in captive chimpanzees during the production of learned vocalizations, suggesting that control of such orofacial movements is lateralized to the left hemisphere. Future studies are needed to investigate the potential relationship between asymmetry of Broca's area in nonhuman primates and lateralization of a diversity of communicative orofacial movements.

Because of the strong population-wide trend toward leftward lateralization of language representation in the cerebral cortex of humans, hemispheric asymmetry of Broca's area has been a major focus of research. Many different structural parameters have been reported to be asymmetric in Broca's area of humans, although there is a lack of consensus regarding their direction and consistency (reviewed in Schenker et al. 2007; Keller et al. 2009). In a study most directly comparable to the current one, Uylings et al. (2006) performed a stereological analysis of 10 human brains and reported that the volume and total number of neurons in area 44 were significantly larger in the left hemisphere. In area 45, they also found leftward asymmetry; however, the degree of lateralization was only significant among females. In contrast to these results, we did not find evidence of asymmetry in areas 44 and 45 in chimpanzees. This suggests that a major evolutionary shift in human brain organization involved increasing asymmetry of these inferior frontal areas. To explore this possibility further, we compiled data from the literature and calculated the fold difference, without accounting for allometric scaling, between the volumes of several cortical areas in humans versus chimpanzees (Table 7). As a frame of reference, we found that overall brain size in humans is 3.6 times larger than chimpanzees and the whole frontal cortex is 4.6 times larger. In

Table 7
Rank ordered fold difference between brain structure volumes in humans and chimpanzees

Structure	Human versus chimpanzee fold difference	Data source
Brain	3.6	Chimpanzee (n = 12)—the present study; human (n = 10)—Uylings et al. (2006)
Neocortical gray	4.0	Chimpanzee (n = 6) and human (n = 6)—Rilling and Insel (1999)
Frontal cortex	4.6	Chimpanzee (n = 6) and human (n = 10)—Semendeferi et al. (2002)
Area 44 left	6.6	Chimpanzee (n = 12)—the present study; human (n = 10)—Uylings et al. (2006)
Area 10 right	6.3	Chimpanzee (n = 1) and human (n = 1)—Semendeferi et al. (2001)
Area 45 left	6.0	Chimpanzee (n = 12)—the present study; human (n = 10)—Uylings et al. (2006)
Area 45 right	5.0	Chimpanzee (n = 12)—the present study; human (n = 10)—Uylings et al. (2006)
Area 44 right	4.1	Chimpanzee (n = 12)—the present study; human (n = 10)—Uylings et al. (2006)
Area V1 left	1.8	Chimpanzee (n = 7) and human (n = 10)—de Sousa (2008)
Area 13 right	1.4	Chimpanzee (n = 1) and human (n = 1)—Semendeferi et al. (1998)

Note: All data are from either in vivo MRI or shrinkage-corrected measurements of histological sections.

comparison to these structures, left area 44 is 6.6 times larger in humans than in chimpanzees and left area 45 is 6.0 times larger. Because areas 44 and 45 in the left hemisphere are among the most greatly expanded cortical areas yet identified in humans, this evidence supports the conclusion that enlargement of Broca's area on the left side is an evolutionary specialization.

The current findings based on histological definition of areas 44 and 45 may appear to contradict previous results based on MRI measurements showing population-level left hemisphere dominant asymmetry in the surface area of the IFG of African great apes (Cantalupo and Hopkins 2001) and the length of the fronto-orbital sulcus in chimpanzees (Hopkins and Cantalupo 2004). Furthermore, a recent study using voxel-based morphometry in chimpanzees also found significant leftward bias in gray matter density within the IFG operculum (Hopkins et al. 2008). One possible explanation for this apparent incongruity is that the relatively small sample size used in the current histological investigation limited our ability to demonstrate asymmetry at the level of statistical significance. It should be noted, however, that the stereological study of Uylings et al. (2006) in humans, which included an even smaller sample size, was able to statistically detect left hemisphere dominance. Though we failed to find any population-level asymmetries, the interindividual variability was high. For example, 5 out of 6 males were leftward asymmetric for area 44 volume, whereas 5 out of 6 females had a rightward dominance. Thus, it is possible that a larger sample size would reveal significant interactions between asymmetry and sex. Nevertheless, if population-level asymmetries of areas 44 and 45 exist in chimpanzees, they are less robust than in humans. An additional possibility is that morphological asymmetries of the chimpanzee IFG may not be driven by interhemispheric differences in cytoarchitectural boundaries or neuron number. Indeed, such a relationship between asymmetry of MRI-based measures of the IFG and the underlying volume of areas 44 and 45 has not been evaluated or established in humans (Keller et al. 2009). Therefore, as an alternative explanation, we suggest that population-level morphological asymmetry of the IFG in chimpanzees (Cantalupo and Hopkins 2001; Hopkins et al. 2008) may be related to hemispheric differences in the volume of IFG white matter rather than gray matter. Furthermore, asymmetry in the length of IFG sulci might be caused by lateralization in the strength of connections made by local association fibers. Parcellation of the IFG in humans using diffusion tensor tracing shows that connectivity often divides the gyrus along major sulci (Anwander et al. 2007).

We propose a scenario where a leftward asymmetry in the connectivity and/or volume of white matter underlying the IFG was already established at an earlier stage in ape evolution. This asymmetry of connectivity may be functionally linked to lateralization of certain orofacial movements and communicative gestures that are shared in common by humans and other primates. More recently in human evolution, an increase in the gray matter volume of areas 44 and 45 in the left hemisphere accompanied the evolution of language as this area received greater inputs from regions of the temporal cortex conveying lexical and semantic information (Rilling et al. 2008) and became reorganized to operate over more complex hierarchical syntactic computations (Friederici et al. 2006).

The present study provides an important step toward defining the anatomical characteristics of Broca's area that might contribute to this region's involvement in linguistic processes in humans. Further comparative research that examines phenotypic differences between humans and other species in the cytoarchitecture, connectivity, and molecular biology of Broca's area homologue is critical to articulate how our species-specific capacity for language evolved.

Funding

National Science Foundation (BCS-0515484, BCS-0549117, BCS-0824531, DGE-0801634); National Institutes of Health (NS 42867); and the James S. Mc Donnell Foundation (22002078).

Notes

Some of the brains used in this study were loaned by the Great Ape Aging Project and the Foundation for Comparative and Conservation Biology. We thank Drs T. Naidich, B. Delman, and C. Tang for assistance with MRI and K. Gupta for assistance in digitizing images of histological sections. *Conflict of Interest:* None declared.

Address correspondence to Chet C. Sherwood, Department of Anthropology, The George Washington University, 2110 G Street NW, Washington, DC 20052, USA. Email: sherwood@gwu.edu.

References

Aboitiz F, Garcia R, Brunetti E, Bosman C. 2006. The origin of Broca's area and its connections from an ancestral working memory network. In: Grodzinsky Y, Amunts K, editors. Broca's region. Oxford: Oxford University Press. p. 3–16.

Amunts K, Schleicher A, Burgel U, Mohlberg H, Uylings HB, Zilles K. 1999. Broca's region revisited: cytoarchitecture and intersubject variability. J Comp Neurol. 412:319–341.

Amunts K, Schleicher A, Ditterich A, Zilles K. 2003. Broca's region: cytoarchitectonic asymmetry and developmental changes. J Comp Neurol. 465:72–89.

Amunts K, Weiss PH, Mohlberg H, Pieperhoff P, Eickhoff S, Gurd JM, Marshall JC, Shah NJ, Fink GR, Zilles K. 2004. Analysis of neural mechanisms underlying verbal fluency in cytoarchitectonically defined stereotaxic space—the roles of Brodmann areas 44 and 45. Neuroimage. 22:42–56.

Anwander A, Tittgemeyer M, von Cramon DY, Friederici AD, Knosche TR. 2007. Connectivity-based parcellation of Broca's area. Cereb Cortex. 17:816–825.
Arbib MA. 2005. From monkey-like action recognition to human language: an evolutionary framework for neurolinguistics. Behav Brain Sci. 28:105–167.
Bailey P, von Bonin G, McCulloch WS. 1950. The isocortex of the chimpanzee. Urbana (IL): University of Illinois Press.
Bookheimer S. 2002. Functional MRI of language: new approaches to understanding the cortical organization of semantic processing. Annu Rev Neurosci. 25:151–188.
Burton MW. 2001. The role of inferior frontal cortex in phonological processing. Cogn Sci. 25:695–709.
Cabeza R, Nyberg L. 2000. Imaging cognition II: an empirical review of 275 PET and fMRI studies. J Cogn Neurosci. 12:1–47.
Cantalupo C, Hopkins WD. 2001. Asymmetric Broca's area in great apes. Nature. 414:505.
Caplan D. 2001. Functional neuroimaging studies of syntactic processing. J Psycholinguist Res. 30:297–320.
Connolly CJ. 1950. The external morphology of the primate brain. Springfield (IL): C.C. Thomas.
de Sousa AA. 2008. Hominoid brain organization: histometric and morphometric comparisons of visual brain structures [PhD Dissertation]. Washington (DC): The George Washington University.
Duvernoy J. 1991. The human brain: surface, three-dimensional sectional anatomy and MRI. Vienna (Austria): Springer-Verlag.
Fadiga L, Craighero L. 2006. Hand actions and speech representation in Broca's area. Cortex. 42:486–490.
Falzi G, Perrone P, Vignolo LA. 1982. Right-left asymmetry in anterior speech region. Arch Neurol. 39:239–240.
Ferrari PF, Gallese V, Rizzolatti G, Fogassi L. 2003. Mirror neurons responding to the observation of ingestive and communicative mouth actions in the monkey ventral premotor cortex. Eur J Neurosci. 17:1703–1714.
Fernández-Carriba S, Loeches A, Morcillo A, Hopkins WD. 2002. Asymmetry in facial expression of emotions by chimpanzees. Neuropsychologia. 40:1523–1533.
Fischl B, Rajendran N, Busa E, Augustinack J, Hinds O, Yeo BTT, Mohlberg H, Amunts K, Zilles K. 2007. Cortical folding patterns and predicting cytoarchitecture. Cereb Cortex. 18:1973–1980.
Foundas AL. 2001. The anatomical basis of language. Top Lang Disord. 21:1–19.
Foundas AL, Eure KF, Luevano LF, Weinberger DR. 1998. MRI asymmetries of Broca's area: the pars triangularis and pars opercularis. Brain Lang. 64:282–296.
Foundas AL, Leonard CM, Gilmore RL, Fennell EB, Heilman KM. 1996. Pars triangularis asymmetry and language dominance. Proc Natl Acad Sci USA. 93:719–722.
Friederici AD, Bahlmann J, Heim S, Schubotz RI, Anwander A. 2006. The brain differentiates human and non-human grammars: functional localization and structural connectivity. Proc Natl Acad Sci USA. 103:2458–2463.
Gallyas F. 1971. A principle for silver staining of tissue elements by physical development. Acta Morphol Acad Sci Hung. 19:57–71.
Gil-da-Costa R, Martin A, Lopes MA, Munoz M, Fritz JB, Braun AR. 2006. Species-specific calls activate homologs of Broca's and Wernicke's areas in the macaque. Nat Neurosci. 9:1064–1070.
Gompertz RHC. 1902. Specific gravity of the brain. J Physiol. 27:459–462.
Gundersen HJ, Jensen EB, Kieu K, Nielsen J. 1999. The efficiency of systematic sampling in stereology—reconsidered. J Microsc. 193:199–211.
Gundersen HJG, Bagger P, Bendtsen TF, Evans SM, Korbo L, Marcussen N, Moller AM, Nielsen K, Nyengaard JR, Paakenberg B, et al. 1988. The new stereological tool: disector, fractionator, nucleator and point sampled intercepts and their use in pathological research and diagnosis. Acta Pathol Microbiol Immunol Scand. 96:857–881.
Hauser MD, Chomsky N, Fitch WT. 2002. The faculty of language: what is it, who has it, and how did it evolve? Science. 298: 1569–1579.
Hauser MD, Marler P. 1993. Food-associated calls in rhesus macaques (*Macaca mulatta*): I. Socioecological factors influencing call production. Behav Ecol. 4:194–205.
Heim S, Eickhoff SB, Amunts K. 2008. Specialisations in Broca's region for semantic, phonological, and syntactic fluency? Neuroimage. 40:1362–1368.
Hook-Costigan MA, Rogers LJ. 1998. Lateralized use of the mouth in production of vocalizations by marmosets. Neuropsychologia. 36:1265–1273.
Hopkins WD. 1995. Hand preferences for a coordinated bimanual task in 110 chimpanzees (*Pan troglodytes*): cross-sectional analysis. J Comp Psychol. 109:291–297.
Hopkins WD. 2007. Hemispheric specialization in chimpanzees evolution of hand and brain. In: Shackelford T, Keenan JP, Platek SM, editors. Evolutionary cognitive neuroscience. Boston (MA): MIT Press. p. 95–120.
Hopkins WD, Cantalupo C. 2004. Handedness in chimpanzees (*Pan troglodytes*) is associated with asymmetries of the primary motor cortex but not with homologous language areas. Behav Neurosci. 118:1176–1183.
Hopkins WD, Taglialatela JP, Meguerditchian A, Nir T, Schenker NM, Sherwood CC. 2008. Gray matter asymmetries in chimpanzees as revealed by voxel-based morphometry. Neuroimage. 42:491–497.
Karlen SJ, Krubitzer L. 2006. Phenotypic diversity is the cornerstone of evolution: variation in cortical field size within short-tailed opossums. J Comp Neurol. 499:990–999.
Keller SS, Highley JR, Garcia-Finana M, Sluming V, Rezaie R, Roberts N. 2007. Sulcal variability, stereological measurement and asymmetry of Broca's area on MR images. J Anat. 211:534–555.
Keller SS, Crow T, Foundas A, Amunts K, Roberts N. 2009. Broca's area: nomenclature, anatomy, typology and asymmetry. Brain Lang. 109:29–48.
Knecht S, Dräger B, Deppe M, Bobe L, Lohmann H, Flöel A, Ringelstein E-B, Hennigsen H. 2000. Handedness and hemispheric language dominance in healthy humans. Brain. 123:2512–2518.
Kreht H. 1936. Architektonik der Brocaschen Region beim Schimpansen und Orang-Utan. Ztschr Anat Entwicklungesch. 105:654–677.
Losin EAR, Russell JL, Freeman H, Meguerditchian A, Hopkins WD. 2008. Left hemisphere specialization for oro-facial movements of learned vocal signals by captive chimpanzees. PLoS ONE. 3:e2529.
Ojemann GA. 1991. Cortical organization of language. J Neurosci. 11:2281–2287.
Ono M, Kubik S, Adernathey CD. 1990. Atlas of the cerebral sulci. New York: Thieme.
Parr LA, Heckt E, Barks SK, Preuss TM, Votaw JR. 2009. Face processing in the chimpanzee brain. Curr Biol. 19:50–53.
Petrides M, Cadoret G, Mackey S. 2005. Orofacial somatomotor responses in the macaque monkey homologue of Broca's area. Nature. 435:1235–1238.
Petrides M, Pandya DN. 2001. Comparative cytoarchitectonic analysis of the human and the macaque ventrolateral prefrontal cortex and corticocortical connection patterns in the monkey. Eur J Neurosci. 16:291–310.
Rilling JK, Insel TR. 1999. The primate neocortex in comparative perspective using magnetic resonance imaging. J Hum Evol. 37:191–223.
Rilling JK, Barks SK, Parr LA, Preuss TM, Faber TL, Pagnoni G, Bremner JD, Votaw JR. 2007. A comparison of resting-state brain activity in humans and chimpanzees. Proc Natl Acad Sci USA. 104:17146–17151.
Rilling JK, Glasser MF, Preuss TM, Ma X, Zhao T, Hu X, Behrens T. 2008. The evolution of the arcuate fasciculus revealed with comparative DTI. Nat Neurosci. 11:382–384.
Schenker NM, Buxhoeveden DP, Blackmon WL, Amunts K, Zilles K, Semendeferi K. 2008. A comparative quantitative analysis of cytoarchitecture and minicolumnar organization in Broca's area in humans and great apes. J Comp Neurol. 510:117–128.
Schenker NM, Sherwood CC, Hof PR, Semendeferi K. 2007. Microstructural asymmetries of the cerebral cortex in humans and other mammals. In: Hopkins WD, editor. The evolution of hemispheric specialization in primates. San Diego (CA): Academic Press. p. 91–116.

Schmitz C, Hof PR. 2000. Recommendations for straightforward and rigorous methods of counting neurons based on a computer simulation approach. J Chem Neuroanat. 20:93–114.
Semendeferi K, Armstrong E, Schleicher A, Zilles K, Van Hoesen GW. 1998. Limbic frontal cortex in hominoids: a comparative study of area 13. Am J Phys Anthropol. 106:129–155.
Semendeferi K, Armstrong E, Schleicher A, Zilles K, Van Hoesen GW. 2001. Prefrontal cortex in humans and apes: a comparative study of area 10. Am J Phys Anthropol. 114:224–241.
Semendeferi K, Lu A, Schenker N, Damasio H. 2002. Humans and great apes share a large frontal cortex. Nat Neurosci. 5:272–276.
Sherwood CC, Broadfield DC, Holloway RL, Gannon PJ, Hof PR. 2003. Variability of Broca's area homologue in African great apes: implications for language evolution. Anat Rec. 271A:276–285.
Shu S, Ju G, Fan L. 1988. The glucose oxidase-DAB-nickel method in peroxidase histochemistry of the nervous system. Neurosci Lett. 85:169–171.
Springer JA, Binder JR, Hammeke TA, Swanson SJ, Frost JA, Bellgowan PS, Brewer CC, Perry HM, Morris GL, Mueller MW. 1999. Language dominance in neurologically normal and epilepsy subjects. Brain. 122:2033–2046.
Taglialatela J, Russell J, Schaeffer J, Hopkins W. 2008. Communicative signaling activates 'Broca's' homolog in chimpanzees. Curr Biol. 18:343–348.
Taglialatela JP, Cantalupo C, Hopkins WD. 2006. Gesture handedness predicts asymmetry in the chimpanzee inferior frontal gyrus. Neuroreport. 17:923–927.
Taglialatela JP, Russell JL, Schaeffer JA, Hopkins WD. 2009. Visualizing vocal perception in the chimpanzee brain. Cereb Cortex. 19:1151–1157.
Uylings HB, Jacobsen AM, Zilles K, Amunts K. 2006. Left-right asymmetry in volume and number of neurons in adult Broca's area. Cortex. 42:652–658.
Van der Gucht E, Youakim M, Arckens L, Hof PR, Baizer JS. 2006. Variations in the structure of the prelunate gyrus in Old World monkeys. Anat Rec. 288A:753–775.
Watanabe-Sawaguchi K, Kubota K, Arikuni T. 1991. Cytoarchitecture and intrafrontal connections of the frontal cortex of the brain of the hamadryas baboon (*Papio hamadryas*). J Comp Neurol. 311:108–133.
West MJ, Slomianka L, Gundersen HJG. 1991. Unbiased stereological estimation of the total number of neurons in the subdivisions of the rat hippocampus using the optical fractionator. Anat Rec. 231:482–497.